JOURNAL OF AIRCRAFT
Vol. 43, No. 5, September–October 2006

Engineering Notes

ENGINEERING NOTES are short manuscripts describing new developments or important results of a preliminary nature. These Notes should not exceed 2500 words (where a figure or table counts as 200 words). Following informal review by the Editors, they may be published within a few months of the date of receipt. Style requirements are the same as for regular contributions (see inside back cover).

Tip Vortex Dependence with Angle of Attack

David H. May* and Georgios H. Vatistas†
Concordia University, Montreal, Quebec H3G 1M8, Canada

DOI: 10.2514/1.22839

Nomenclature

a_o = lift slope
b = span
c = wing cord
C_L = lift coefficient, $L/0.5\rho U_\infty^2 cb$
F_3 = function of x/c and Re
F_{12} = function of TG* and Re_θ
G = function of r^*, also designated $G(r^*)$
K_1 = $(1 - \Delta P_t)/(1/2\rho U_\infty^2)$
K_2 = $V(r^* = 0)$
L = lift
m = value of exponent, 0.5
r = radial distance from the vortex center
r_c = vortex core radius
r^* = r/r_c
Re = Reynolds number, $U_\infty c/\nu$
Re_θ = $v_\theta r_c/\nu$
TG = characteristic tip geometry, units of area
TG* = TG/cb
u = axial component of velocity
$u_{\max}$ = maximum axial component of velocity
U_∞ = free stream velocity
V = axial jet function
v_θ = tangential component of velocity
$v_{\theta,\max}$ = maximum tangential component of velocity
x = streamwise distance from a virtual origin of tip vortex creation
α_E = effective angle of attack, geometric angle of attack minus zero lift angle of attack
α^* = function of α_E/F_3
β = parameter that is proportional to the root circulation, defined in [1]
Γ = circulation
Γ_c = core circulation
Γ_o = vortex circulation
ΔH = loss, defined in [11]
ΔP_t = total pressure loss
η = transformed variable, α_E/F_3
ν = kinematic viscosity
ξ = transformed variable, $\alpha_E^m F_{12}$
ρ = density

Received 30 January 2006; revision received 14 April 2006; accepted for publication 14 April 2006.

*Research Assistant, Department of Mechanical and Industrial Engineering, 1455 de Maisonneuve Boulevard West, H549 Montreal.
†Professor, Department of Mechanical and Industrial Engineering, 1455 de Maisonneuve Boulevard West, H549 Montreal. Senior Member AIAA.

Introduction

THE fundamental methodology in the design of a lifting surface is that if the fluid on the upper surface goes quicker than that of the lower surface, then lift will be generated. For a very long wing (high aspect ratio), the pressure distributions at any spanwise station should be identical, but for the fluid in the vicinity of the wing tip, there is an inherent three-dimensionality to the flow. In this region the flow senses the pressure gradient, as imposed by the center portion of the wing, and as a result, there is a secondary component of flow in the direction of this gradient.

This is the basic underlying process; however, there are many details to this process, which are yet to be fully understood. This note develops the dependence between the tip vortex and the angle of attack of a thin wing.

Asymptotic Regimes

In 1972, Moore and Saffman et al. [1,2] produced a theory describing the variation of vortex characteristics with wing loading and downstream position. Their work was restricted to laminar flows with low wing loading where the axial velocity perturbation is small. Then, the tangential velocity decays, following the expression

$$v_{\theta,\max} = 0.49\beta(x/c)^{-0.25} Re^{-0.25} \tag{1}$$

Additionally, for a large aspect ratio (or large loading), thin wing, at small angle of attack, β varies linearly with angle of attack. Assuming self-similarity of the vortex profile, Eq. (1) can then be generalized as

$$\frac{v_\theta}{U_\infty} = \frac{\alpha_E}{F_3} G(r^*) \tag{1b}$$

It is desirable to obtain the dependence of the vortex with angle of attack, as the tangential velocity becomes very large.

Or,

$$v_\theta \gg U_\infty$$

Listing all variables and parameters of primary importance a general functional relationship is constructed:

$$v_\theta = \mathrm{fn}(r, r_c; L, \rho, \nu, cb, \mathrm{TG})$$

For the time being we have placed only one characteristic parameter describing the geometry of the tip, and have designated it to be TG. It may be assumed that its dimensions are that of either length or area. Also, the main source of shear stress is due to the molecular, kinematic viscosity, and for this reason the only flow parameter will be the Reynolds number; this will be generalized subsequently. Understanding that four dimensionless groups are sufficient (the core radius is a variable that is expressed as a function of all other variables), we shall restrict ourselves to cases that scale as follows.

$$\frac{\rho v_\theta^2 cb}{L} = \text{fn}(Re_\theta, \text{TG}^*, r^*) \tag{2}$$

Consequently, the streamwise velocity does not scale with the tangential velocity because the magnitude of the tangential velocity is so great that a variation in streamwise velocity is negligible (except in implicitly maintaining the lift). Then, by dimensional necessity, the square tangential velocity must scale with lift. The pressure gradient (as produced by lift) is the driver of the tangential component of velocity and if it were not present the tangential velocity would, identically, be zero. By analogy, when considering the flow around a sharp bend in a channel, the streamlines are like those of the streamlines of the tip vortex projected in the crossflow plane [3].

The characteristic dimension of the tip scales with the planform area. Any subsequent tip dimensions that would be included in the analysis would need to scale with this, or possibly, with a previously defined tip characteristic.

There is no dependence on the aspect ratio. Because the loading is heavy, the sectional lift coefficient towards the center of the wing is approximately constant; in this case, the effect (on the tip vortex) of further increasing the span is negligible.

The radial direction has been modeled to scale with the core radius, the location of maximum velocity. In the near field, unfortunately, this self-similarity is not as strong as what is observed far away from the point of tip vortex genesis. This lack of perfect coherency results from the presence of another characteristic geometry, namely, the wing. For this reason, values of core radius and peak tangential velocity cited in the preceding expressions could correspond to the circumferentially averaged values when compared with the experimentally observed quantities.

We assume a low enough angle of attack, such that

$$C_L = a_o \alpha_E$$

Also, assuming that separation of variables is possible, and that the tangential velocity profile shape has not significantly changed from the near to far field regime. Under these assumptions, expression (2) takes on the relatively simple form

$$\frac{v_\theta}{U_\infty} = \alpha_E^{0.5} F_{12} G(r^*) \tag{2b}$$

The square root variation serves as an asymptotic state. If there was flow only in the crossflow plane (with the same pressure gradient being applied) it would be satisfied exactly; however, when there is an increased presence of the streamwise component the value of the exponent increases until it reaches another asymptote, of linear scaling, as obtained in the work of Moore and Saffman [1]. Because the first regime of square root scaling requires higher tangential velocities, it is approached when we are closer to the wing, before the decay process has taken effect, and also as the lift, and thus, angle of attack, is increased (but still below its stalling condition). The second regime of linear scaling is approached far away or at low angle of attack. Examples of the velocity profiles dependence with angle of attack can be found in [4–8] and can be shown to all scale with different exponents, all varying between 1 and 0.5.

Intermediate Regime

Now that the lower and upper asymptotes have been obtained, it remains to match these two conditions, such that a region where these two regimes are in balance is obtained.

Restating the results of the preceding section,

$$\frac{v_\theta}{U_\infty} = \alpha_E^m F_{12} G = \xi G$$

and

$$\frac{v_\theta}{U_\infty} = \frac{\alpha_E}{F_3} G = \eta G$$

express the asymptotic near-field regime and the asymptotic far-field regime, respectively. Then a deviation from the far-field regime could be well modeled by

$$\frac{v_\theta}{U_\infty} = f(\eta) G \tag{3a}$$

and a deviation from the near-field regime could be well modeled by

$$\xi G - \frac{v_\theta}{U_\infty} = g(\xi) G \tag{3b}$$

For conditions that are in balance with these two regimes, we should expect

$$f(\eta) = \xi - g(\xi)$$

Taking the derivative with respect to α_E and then multiplying by α_E we obtain

$$\frac{\partial f(\eta)}{\partial \eta} \eta = m \left(\xi - \frac{\partial g(\xi)}{\partial \xi} \xi \right)$$

We observe that the left hand side is, at most, solely a function of η, and the right hand side is, at most, solely a function of ξ. Under these conditions, both sides are actually equal to a constant. For this reason, the two sides of the equations may be separated and integrated to obtain

$$f(\eta) = K \ell_n(\eta) + B, \qquad g(\xi) = \xi - \frac{K}{m} \ell_n(\xi) + A$$

Inserting into (3a) and (3b), this yields two separate, but equivalent, expressions for the tangential velocity,

$$\frac{v_\theta}{U_\infty} = \left(\frac{K}{m} \ell_n(\xi) - A \right) G = [K \ell_n(\eta) + B] G$$

A, B, and K are all "pure" constants. Expressing the velocity in terms of the far-field variables, η is more convenient because, at a given stream Reynolds number, it is clear that the far-field variable varies linearly with angle of attack (recall F_{12} is a function of $v_\theta \ldots$ etc., which vary with angle of attack).

Under some conditions, perhaps other flow parameters are needed to sufficiently describe the test conditions, namely, a turbulence parameter. Observe that there are two minimum requirements for the preceding model to apply; they are

1) that the near field and the far field have different scaling, with angle of attack; this was demonstrated in the cited references to be a fundamental quality.

2) that the near field and far field scale with different variables (or functions), what has been called F_{12} and F_3. This can be easily satisfied by the fact that in the near field the tip vortex is a function of the specific tip geometry, whereas far away from the wing the tip vortex should only feel the effective "lifting line," which is solely a function of the wing planform shape and not the tip shape.

Results

Based on the results of the preceding sections, the far-field and intermediate-field regimes may be generalized as taking on the form

$$\frac{v_\theta}{U_\infty} \frac{1}{G} = \alpha^* \tag{4a}$$

where $\alpha^* = \alpha_E / F_3$ in the far field and $\alpha^* = K \ell_n(\alpha_E / F_3) + B$ in the intermediate regime.

Evaluating (4a) at its maximum $v_\theta = v_{\theta,\max}, G(r^*) = G(1)$, we obtain

$$\frac{v_{\theta,\max}}{U_\infty} \frac{1}{G(1)} = \alpha^* \tag{4b}$$

Data presented in Fig. 1 display the value of (4b) in all three regimes. The constants K and B can be assessed from such a sample.

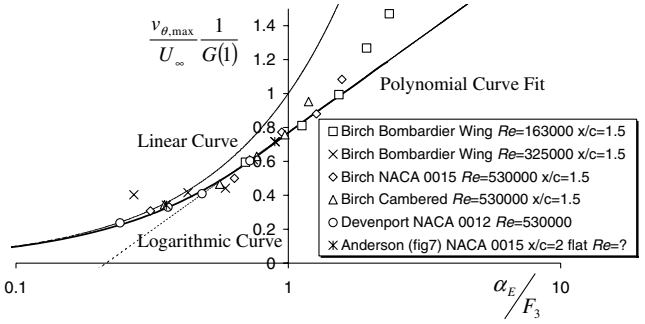

Fig. 1 Variation of core tangential velocity with angle of attack.

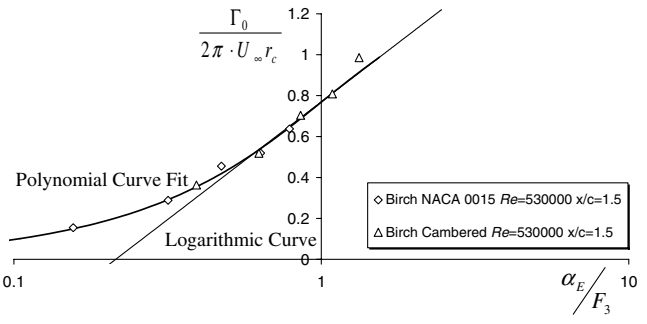

Fig. 2 Variation of vortex intensity with angle of attack.

It is a relatively easy matter to assess the value of K, which is found to be $K \cong 0.5$. The value of B is much more difficult to approximate (and probably much less "universal"), but is approximated at $B \cong 0.77$. As the angle of attack is decreased or the streamwise distance and Reynolds number increased the points can be expected to "slide down" the curve until the asymptotic, low wing loading solution of Moore and Saffman [1] is reached.

A curve fit spanning the entire near- and far-field regime is

$$\alpha^* = \frac{\alpha_E}{F_3} + \sum_{i=2}^{6} a_i \left(\frac{\alpha_E}{F_3}\right)^i$$

The symbolic expression for the coefficients, and how they are obtained, can be found in the thesis by May [9]. When we plug in $K = 0.5$ and $B = 0.77$ we obtain the numerical values of the coefficient presented in Table 1.

The circulation at a given radial location is calculated and evaluated at any multiple of the core radius to give

$$\Gamma = 2\pi U_\infty r_c \alpha^* G(r^*) r^* \tag{5}$$

If the vortex profile far away from the origin is $G(r^*) = 1/r^*$, then

$$\frac{\Gamma_0}{2\pi U_\infty r_c} = \alpha^* \tag{6}$$

If the left hand side is plotted for a given wing, Reynolds number, and streamwise location, the same variation with angle of attack should be obtained as the one that was obtained with the tangential velocity; see Fig. 2.

We can use the expression in (6) to nondimensionalize the circulation in (5) to yield

$$\Gamma/\Gamma_0 = G(r^*) r^*$$

which shows that our results are indeed consistent with that of an idealized vortex model like those of Vatistas [10] or Lamb [11]. Also we observe that

$$\Gamma_c/\Gamma_0 = G(1)$$

This value was obtained in curve fitting the maximum velocity in Eq. (4b). As a result of this we may write an expression for the maximum velocity as

$$\frac{v_{\theta,\max}}{U_\infty} = (\Gamma_c/\Gamma_0)\alpha^*$$

Table 1 Polynomial curve fit parameters

Parameter	Value
a_2	−0.3245
a_3	0.315528
a_4	−0.3709
a_5	0.176842
a_6	−0.02865

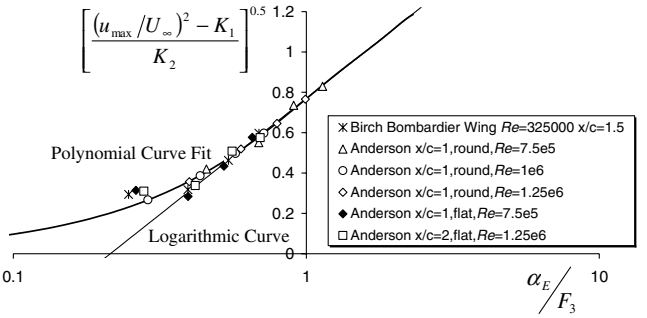

Fig. 3 Variation of axial velocity with angle of attack.

Batchelor's analysis [12] of axial flow in a trailing vortex is still used to this day (see Spalart [13] or Anderson and Lawton [14]); the model can display velocity excess or deficit yet has no explicit mechanism to explain the effect of angle of attack.

Batchelor's equation for the axial velocity is

$$u^2 = U_\infty^2 + \int_r^\infty \frac{1}{(2\pi r)^2}\frac{\partial(\Gamma^2)}{\partial r}\,\mathrm{d}r - 2\Delta H$$

This expression can be put into a more convenient form by inserting the expression for the circulation in (5). Defining

$$V = \int_{r^*}^\infty 1/r^{*2}\frac{\mathrm{d}}{\mathrm{d}r^*}[G(r^*)r^*]\,\mathrm{d}r^*$$

we obtain

$$\left(\frac{u}{U_\infty}\right)^2 = \left(1 - \frac{\Delta P_t}{\frac{1}{2}\rho U_\infty^2}\right) + V\alpha^{*2}$$

In the restricted case that the total pressure loss is relatively constant over a range of angles of attack, it should be possible to curve fit maximum axial velocity data to the form

$$\left[\frac{(u_{\max}/U_\infty)^2 - K_1}{K_2}\right]^{0.5} = \alpha^*$$

where $K_1 = (1 - \Delta P_t)/(1/2\rho U_\infty^2)$ and $K_2 = V(r^* = 0)$ are curve fitted values.

From Fig. 3 we see that this rule is observed to sometimes hold. There is difficulty in the low angle-of-attack region to conform to the curve, surely because the total pressure loss must drop to zero as the angle of attack is decreased or as we increase distance from the wing (increasing F_3).

Conclusion

An analysis that explains the dependence of the tip vortex characteristics and their variation with angle of attack and downstream distance, under certain conditions, has been detailed. First, the low wing loading analysis of Moore and Saffman [1] is used as the asymptotic far-field regime. Dimensional analysis presents

reasoning for a hypothetical near field. A balance of these two scaling laws is made and is shown to apply in an intermediate-field regime. In the intermediate field, various vortex characteristics are shown to vary as a logarithmic variation with angle of attack. The expressions obtained are shown to hold for some peak tangential velocity data. An expression coupling the circulation and the core radius is obtained. This is used to obtain an expression for the axial velocity; under the assumption of constant total pressure losses over a range of angle of attack, the expression obtained is shown to be in agreement with some experimental data.

References

[1] Moore, D. W., and Saffman, P. G., "Axial Flow in Laminar Trailing Vortices," *Proceedings of the Royal Society of London A*, Vol. 333, June 1973, pp. 491–508.

[2] Baker, G. R., Barker, S. J., Bofah, K. K., and Saffman, P. G., "Laser Anemometer Measurements of Trailing Vortices in Water," *Journal of Fluid Mechanics*, Vol. 65, Pt. 2, 1974, pp. 325–336.

[3] Francis, M. S., and Kennedy, D. A., "Formation of a Trailing Vortex," *Journal of Aircraft*, Vol. 16, No. 3, 1979, pp. 148–154.

[4] Devenport, W. J., Rife, M. C., and Liapis, S. I., "Structure and Development of a Wing-Tip Vortex," *Journal of Fluid Mechanics*, Vol. 312, April 1996, pp. 67–106.

[5] Higuchi, H., Quadrelli, J. C., and Farell, C., "Vortex Roll-Up from an Elliptic Wing at Moderately Low Reynolds Numbers," *AIAA Journal*, Vol. 25, No. 12, 1987, pp. 1537–1542.

[6] El-Ramly, Z., and Rainbird, W. J., "Flow Survey of the Vortex Wake Behind Wings," *Journal of Aircraft*, Vol. 14, No. 11, 1977, pp. 1102–1108.

[7] Birch, D., Lee, T., Mokhtarian, F., and Kafyeke, F., "Rollup and Near-Field Behavior of a Tip Vortex," *Journal of Aircraft*, Vol. 40, No. 3, 2003, pp. 603–607.

[8] Birch, D., Lee, T., Mokhtarian, F., and Kafyeke, F., "Structure and Induced Drag of a Tip Vortex," *Journal of Aircraft*, Vol. 41, No. 5, 2004, pp. 1138–1145.

[9] May, D., "Wing Tip Vortex Dependence with Angle of Attack," M.Sc. Dissertation, Concordia Univ., Montreal, 2006.

[10] Vatistas, G. H., Lin, S., and Li, P. M., "Similar Profile for the Tangential Velocity in Vortex Chambers," *Experiments in Fluids*, Vol. 6, No. 2, 1988, pp. 135–137.

[11] Lamb, H., *Hydrodynamics*, 6th ed., Dover, New York, 1945.

[12] Batchelor, B. K., "Axial Flow in Trailing Vortices," *Journal of Fluid Mechanics*, Vol. 20, Pt. 4, 1964, pp. 645–658.

[13] Spalart, P. R., "Airplane Trailing Vortices," *Annual Review of Fluid Mechanics*, Vol. 30, Jan. 1998, pp. 107–138.

[14] Anderson, E. A., and Lawton, T. A., "Correlation Between Vortex Strength and Axial Velocity in a Trailing Vortex," *Journal of Aircraft*, Vol. 40, No. 4, 2003, pp. 699–704.